Characterization of SnO_2 Film with Al-Zn Doping Using Sol-Gel Dip Coating Techniques

IOP Conf. Series: Journal of Physics: Conf. Series **1011** (2018) 012015 doi:10.1088/1742-6596/1011/1/012015

Characterization of SnO_2 Film with Al-Zn Doping Using Sol-Gel Dip Coating Techniques

A Doyan[1], Susilawati[1], N Ikraman[1] , M Taufik[2]

[1]Magister Science, Post Graduate of Mataram University, Mataram, Indonesia
[2]Physics Education Mataram University, Indonesia

Email: arisdoyan@yahoo.co.id

Abstract. Sn $_{1-2x}$ $Al_xZn_xO_2$ film has been developed using sol-gel dip coating technique. The materials $SnCl_2.2H_2O$, $AlCl_3$ and $ZnCl_2$ dissolved in water and ethanol with 5:95 volume ratio. Variations dopant concentration x = 0.000, 0.005, 0.0025, and 0.050. The film was grown with sol concentration 0.4 M, the withdrawal speed of 12 cm/min and sintering at 600 °C for 30 minutes. The characteristics Sn $_{1-2x}$ $Al_xZn_xO_2$ films with various doping concentration phase were characterized by XRD. The morphological characteristics and the composition of the constituent elements of the film were characterized by SEM-EDX. The characteristics of the shape, structure, and size of the particles were characterized by TEM. The XRD results show that all films have a tetragonal SnO_2 rutile phase without any secondary phase with an average particle size in the range 5.14 – 2.09 nm. The SEM results show that the film grown has a smooth morphology with a striped texture (x = 0.00), and there is a crack (x = 0.050). The EDX results show that the composition and distribution of the constituent elements of the film are uniformly distributed. TEM results show that the particle films has tetragonal rutile structure, orthorhombic and amorphous with a spherical shape.

Keywords: Tin oxide, Zinc doping, Al doping, Sol-Gel, Dip Coating

1. Introduction

The tin oxide (SnO_2) is one n-type transparent semiconductor material with a wide energy band gap (~ 3.6 eV), combines high optical transparency and low resistivity that makes this material applied to solar cells, Liquid Crystal Display and other optoelectronic devices. In addition, SnO_2 is very sensitive to the presence of surrounding gas which makes it is applied as gas sensors [1]. Due to its nature and application, the study of SnO_2 engineering is very intensive. The preparation and growth of SnO_2 film can be done with various techniques such as Chemical Vapor Deposition (CVD) [2], DC and RF Sputtering [3], Pulsed Laser Deposition [4], Chemical Bath Deposition [5], and Sol-Gel Spray Pyrolysis [6], Sol-Gel Spin Coating [7], and Sol-Gel Dip Coating [8]. Of all these methods, Sol-Gel Dip Coating is a very good technique, because it is the simplest one that can grow the film on various forms of the substrate, ease in controlling particle growth and doping, and economical addition.

The characteristics of SnO_2 films are known to be enhanced by the addition of doping. Dopants generally have larger or smaller valence electrons with Sn^+, and have a similar ionic radius. Dopants may be of a single element such as Sb, F, Zn, Al, Mn or double-shaped elements such as Sb-F, Zn-Co, and others that depend on the application of SnO_2 itself. The SnO_2 films doped with Zn^{2+} and Al^{3+} ions are known to affect SnO_2 properties themselves, including stabilizing SnO_2 particles and changing energy band gaps, increasing optical transmittance and electrical conductivity, altering structural, increasing responsiveness, selectivity and stability in sensor gas. However, it is not yet known how the effect of these two dopants

combined on the characteristics of the SnO_2 film. So it is necessary to further investigate the effect of these two dopants on the characteristics of the SnO_2 film. Therefore, in this study the growth of the SnO_2 thin film with combined doping of Zn^{2+} and Al^{3+} was done using Dip Coating Sol-Gel.

2. Materials and Methods

The basic ingredients used as the films in this study were as follows Tin (II) chloride dihydrate ($SnCl_2 \cdot 2H_2O$) with molar mass 225.63gr/mol, 98% purity, Merck). The solvent used was Ethanol (C_2H_5OH) with a molar mass of 46.07gr/mol (98% purity, Merck) and Aquades. The dopant material used was Zinc dichloride ($ZnCl_2$) with molar mass 136.30 g/mol (98% purity, Merck) and Aluminum Chloride ($AlCl_3$) with molar mass 133.34 g/mol (98% purity, Merck). The substrate film used is glass preparations with dimensions of 2.54 mm x 76.2 mm x 1 mm. While the material for washing the substrate is Hydrochloride (HCl 1.0 M) and ceramic detergent. The procedure of $Sn_{1-2x}Zn_xAl_xO_2$ sol preparation is a modification of the sol-gel preparation of $SnCl_2.2H_2O$. The $ZnCl_2$ and $AlCl_3$, dissolved in 5 ml of distilled water using a magnetic stirrer for 30 minutes at 80 ° C until the mass composition ratio $SnCl_2.2H_2O$, $ZnCl_2$, $AlCl_3$ with varying concentrations x (m/m) = 0.000, 0.005, 0.025, 0.050. Then 45 ml of ethanol (C_2H_5OH) was added in the mixture solution to obtain a constant solubility concentration of 0.4 mol / L. The solution was then stirred at 80 °C for two hours and kept for two days. The glass substrate before the deposition was washed using detergent followed by substrate soaking for one day in a mixed solution of 100 ml of HCl 1M with 300 ml of distilled water for one day. Then the substrate was washed with flowing distilled water. The substrate is then dried using an oven at 100 °C for one hour [7,9]. Thin layer deposition is done using an instrument with a dip coater pull Speed (Withdrawal Speed) at 12 cm/minute, long soaking 5 seconds, in sintering the electric furnace at a temperature of 600 °C for 30 minutes. This step is done as much as 5 times repetition. The Characterization of $Sn_{1-2x}Zn_xAl_xO_2$ film sample structure was done using XRD Rigaku Smartlab type with Cu Kα radiation. The XRD operating conditions are set at 40.0 kV 30 mA, and the XRD spacer angle range is set at the angle range (2θ) 5°-90°. The morphological characteristics and sample composition are characterized using SEM paired with EDX. In this study, the samples were characterized by samples with doping composition x = 0,000 and 0.050. The regional characterization, size, and regularity of samples were observed using JEOL JEM 1400 TEM. The samples characterized by TEM were samples with dopant composition x = 0.050.

3. Results and Discussion

3.1. Phase and Structure Characteristics

Figure 1 shows the XRD results for $Sn_{1-2x}Zn_xAl_xO_2$ samples at various dopant concentrations. The dopant ions Zn^{2+} and Al^{3+} replaced Sn^{4+} at SnO_2 lattice caused ionic radius Zn^{2+} (0.74 Å) and Al^{3+} (0,5 Å) significantly different with the ionic radius Sn^{4+} (0.69) based of not found the diffraction peaks of Sn, SnO, ZnO and Al_2O_3.These results are similar to other researchers [3, 10]. All samples were oriented to 110, 101, and 211. The addition and increase of Al-Zn dopants increased the intensity of diffraction, except at x = 0.050 which indicated the dopant solubility limit in the lattice SnO_2.

The lattice parameter of the diffraction graph is determined by the equation

$$\frac{1}{d^2} = \left(\frac{h^2 \square k^2}{a^2} \square \frac{l^2}{c^2} \right) \quad [1]$$

The estimated particle size of the film is determined using the Scherer formula

$$D = \frac{K\lambda}{\beta \cos\theta} \quad [2]$$

Where D is the average size of the crystal, K is a constant associated with the crystal form and has a value of 0.9, λ is the X-ray wavelength used (nm), and β represents the peak width at half the maximum diffraction peak (FWHM) (radians).

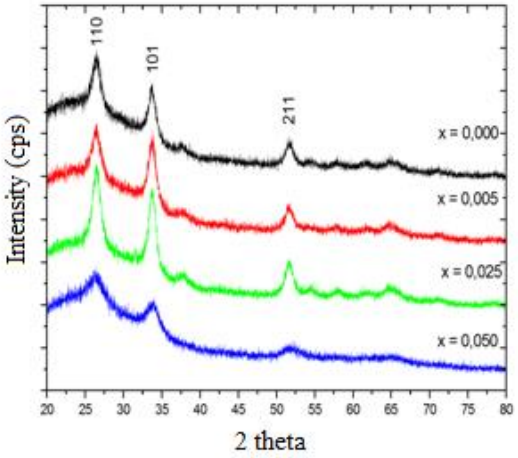

Fig. 1. Graph of the relationship between the diffraction angle with the intensity for variation of doping concentration.

The lattice parameter data and thin film particle size estimation on dopant concentration variations are shown in Table 1.

Table 1. The crystal lattice parameters and particle size of $Sn_{1-2x}Zn_xAl_xO_2$ film

No.	Sample	*a* values (Å)	*c* values (Å)	D (Å)
1.	$x = 0.000$	4.78444	3.18134	51.41
2.	$x = 0.005$	4.75640	3.18336	56.94
3.	$x = 0.025$	4.73352	3.16838	54.78
4.	$x = 0.050$	5.19802	2.93922	20.99

Table 1. shows that the lattice constant a decrease with increasing dopant, but increases drastically at dopant concentration x = 0.050. While the value of c grid constant increased at dopant concentration x = 0.005 which then decreased for dopant concentration x = 0.025 and x = 0.050. This indicates that the substitution of dopant ions Zn^{2+} and Al^{3+} causes SnO_2 lattice distortion caused by the ionic difference of Sn^{4+} radius. The lattice expansion is caused by a Zn^{2+} ionic radius greater than the Sn^{4+} ionic radius, whereas the lattice shrinkage caused by the ionic radius of Al^{3+} is smaller than that of the Sn^{4+} ionic radius which is in agreement with Khan, et al. [11]. This pattern of random lattice constant changes is caused by the substituted dopant replacing the SnO_2 lattice randomly. While at dopant concentration x = 0,050 seen increase of lattice constant a = 5.19802 Å and c = 2.93922 Å close to ZnO lattice constant value. These results indicate that on the axis axes Sn^{4+} ions are replaced with larger Zn^{2+} ions. The particle size of SnO_2 with x = 0.000 is 5.14 nm in the range of 2.67 - 7.76 nm. At dopant concentration x = 0.0050 there was an increase in particle size with an average size of 5.69 nm with a size range of 0.87 - 8.72 nm. At dopant concentration x = 0.025 the particle size decreased with an average size of 5.48 nm with a range of 2.60 - 7.51 nm. At dopant concentration x = 0.050 particle size decreased with mean size 2.09 nm with

range 1.01 - 3,69 nm. The increase in average particle size at low doping concentrations has grown SnO_2 film with Zn doping [12].

3.2. Characteristics of Morphological

The characteristic Film surface morphology is characterized using Scanning Electron Microscope (SEM). FIG. 2 (a) shows the $Sn_{1-2x}Zn_xAl_xO_2$ film image at dopant concentration x = 0,000 textured lines, whereas for dopant concentration x = 0.050 (Fig. 2 (b)) has a smooth surface with two crack types Size 3.27 µm and 0.80 µm and the presence of crater (cater). A crack with a size of 3.27 µm is applied to the previous coating which has been covered by other coatings, whereas a crack with a size of 0.80 µm was observed on the final coating. This crack is due to the high sol high concentration [13] and the high rate of heating at the time of sintering by the electric furnace [14]. Figure 2 (c) shows the transverse incision image of SEM. The films grown have varying thicknesses with a range of 4.37 - 5.00 µm. This thickness is categorized as a thin film [15].

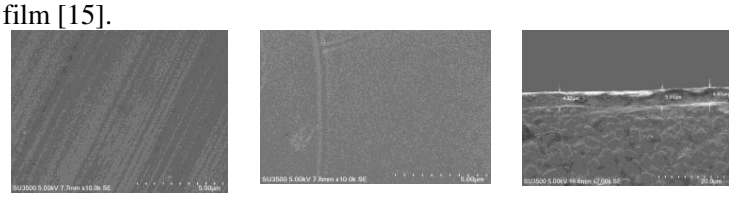

(a) (b) (c)

Fig. 2. The surface morphological image of the film at magnification 10000 times for (a) x = 0.000, (b) x = 0.050, and (c) the transverse incision image of SEM

3.3. Characteristics of Composition

Distribution characteristics and composition of the embedded film material were characterized using the Energy Dispersive X-Ray Spectroscopy (EDX) coupled with the SEM test apparatus. The composition of the film sampling elements for x = 0.000 is indicated by the presence of the energy peaks shown in Fig. 3 (a). The peak at 3.44 and 3.68 eV energy emission from Sn and peak at 0.52 eV represents the energy emission of element O. The pattern of element distribution for a film with x = 0.050 by Fig. 3(b). The peak at energy 0.37, 3.44, 3.66, and 3.94 eV shows the spectra of Sn element. The peak at 0.52 eV shows the spectra of element O. The peak at 1.01, and 1.48 eV shows the dopant elements of Zn and Al. The peaks at 0.25 and 1.74 eV show the spectra of C and Si elements. The presence of C element indicates that the solvent does not evaporate completely, while the Si element in the substrate element (SiO_2).

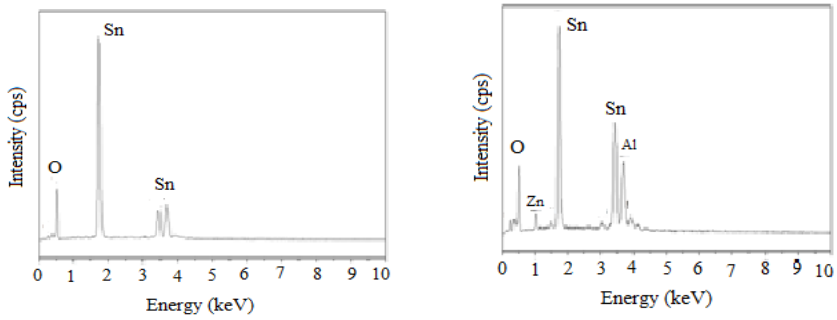

Fig.3. The EDX graph of the film at dopant concentration x = 0.000 dopant and concentration x = 0.050

3.4. Characteristics of Shape and Particle Size

The characteristics of particle shape and size were characterized using TEM. The samples characterized by TEM are samples with doping concentration x = 0.050. The particles are grown spherical with a size range of 3.72 - 6.16 nm. This result differs from the result of particle size estimation with Scherer formula on XRD with particle size range 1.01-3.69 nm (figure 4(a)). TEM can also be used to determine the particle structure through electrons diffraction future in the selected area (Selected Area Diffraction

Electron - SAED). Figure 4(b) shows an irregular pattern of electron diffraction that indicates that some particles have polycrystalline structures with a tetragonal rutile phase with various orientations. This diffraction pattern results in spot irregularities in electron diffraction indicating a lattice disturbance by the Al-Zn dopant corresponding to the XRD results [16]. Figure 4(c) shows that some particles also have polycrystalline structures with orthorhombic phases. The electron diffraction pattern is similar to that of Cd Doped SnO_2 diffraction film grown by Chemical Bath Deposition (CBD) method. The existence of an orthorhombic structure is caused by a lattice distortion caused by a substituted Zn doping ion replacing the SnO_2 lattice, while image 4(d) shows the particles are amorphous. This is due to the nucleation and Growth of imperfect film crystals due to the shortness of sintering time [17].

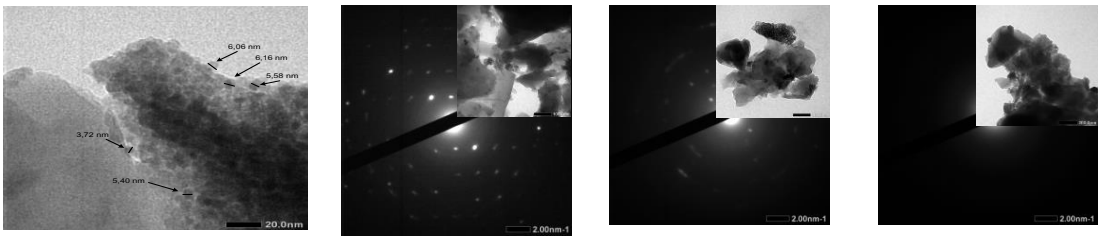

(a) (b) (c) (d)

Fig. 4. Electron Diffraction Pattern Image $Sn_{1-2x}Zn_xAl_xO_2$

4. Conclusion

Results and data analysis can be concluded that the addition of Al-Zn doping does not change the phase SnO_2. The SEM results show that the grown film has a smooth morphology with a striped texture (x = 0,000) and there is a crack (x = 0.050). EDX results show that the constituent elements of the film are spread evenly with the composition according to the calculation. The TEM results show that the film particles have three tetragonal, orthorhombic and amorphous, polycrystalline rutile structures

Acknowledgement

Thank you to all staff and laboratory analytical chemistry Mataram University and laboratory physics Department Institute Technology Bandung and A big thank you to the students the material physics research groups have tried to help prepare samples and data retrieval. We also thanks to the education department of research and technology for the basic research grant in 2017.

References

[1] Batzill M, and Diebol U 2005 The Surface and Materials Science of Tin Oxide *Progress in Surface Science* **79** pp 47–154

[2] Jeong Jin, Choi,Seung Pyung and Hong, Kwang Joon 2006 Structural and Optical Properties of SnO2 Thin Films Deposited by Using CVD Techniques *Journal of the Korean Physical Society*, Vol. **48**, No. 5, May 2006, pp. 960-963

[3] Xu Bo, Ren Xiao-Guang, Gu Guang-Rui, Lan Lei-Lei and Wu Bao-Jia 2016 Structural and optical properties of Zn-doped SnO_2 films prepared by DC and RF magnetron co-sputtering *Superlattices and Microstructures* Volume **89** pp 34-42

[4] Weng Min-Hang, P, Cheng-Tang Y, Ru-Yuan,H, and Chun-Chih, 2011 Structure Optical and Electrical Properties of ZnO Thin Films on The Flexible Substrate by Cathodic Vacuum Arc

Technology with Different Arc Currents *Ceramics International Journal 05,* **43**: 1-6. DOI: 10.1016/j.ceramint.2011.05.043.

[5] Maddu, Akhiruddin, Hasiholan, Rodo Tua, and Kurniati, Mersi 2009 The growth of Nanocrystal SnO_2 film with Chemical Bath Deposition Method (CBD) *Journal of Nanoscience & Nanotechnology* ISSN 1979-0880.

[6] Sriram S and Thayumanavan, A 2013. Effect of Al Concentration on the Optical and Electrical Properties of SnO_2 Thin Films Prepared by Low Cost Spray Pyrolysis Technique *International Journal of Chem. Tech Research* **5**(5): 2204 – 2209.

[7] Doyan, Aris., Susilawati, Imawanti, and Yanika Diah. 2017 Synthesis and characterization of SnO_2 thin layer with a doping aluminum is deposited on quartz substrates *AIP Conference Proceedings* **1801**, 020005 doi: 10.1063/1.4973083

[8] Carvalho, D H Q, Schiavona, M A, Raposoa M T, de Paivaa R, Alvesa, J L A, Paniagob, and Roberto, M 2012 Synthesis and characterization of SnO_2 thin films prepared by dip-coating method *Physics Procedia* **28** 22–27.

[9] Doyan Aris, Susilawati, Fitri S.A Ahzan, Sukainil 2017 Crystal Structure Characterization of Thin Layer Zinc Oxide *IOP Publishing* Ltd, doi: 10.1088/1757-899X/196/1/012016.

[10] De Arijit, 2015 Study of Sol-Gel Derived Spin Cated Cd-Sn Oxide Films on Glass *J. Thin. Film. Sci. Tec.* **4***,* 83-87. DOI: 10.12785/ijtsf/040204.

[11] Khan Z, Raza K M, Shoeb Z, Mohammad K M, Shahid, 2010 Optical and Structural Properties of Thermally Evaporated Cadmium Sulphide Thin Films on Silicon (100) Wafers *Materials Science and Engineering B*., **174**, 1-3: 145-149. DOI: 10.1016/j.mseb.2010.03.006.

[12] Rajwali, K and Ming-Hu F 2015 Dielectric and magnetic properties of (Zn, Co) co-doped SnO_2 nanoparticles *Chinese Physics B* **24**(12), 127803

[13]Uno U E, Emetere M E and Aplha M 2014 Crystalline Grain Size Effects On The Conductivity Of The Doped Tin Dioxide (SnO_2) With Zinc (Zn) *Journal of Ovonic Research* Vol. **10** No. 3 pp 83-88

[13] Miller T A, Bakrania S D, Perez C and Wooldrige M S 2006 Nanostructured Tin Dioxide Materials for Gas Sensor Application *J. F. Nanomaterials* pp 1-24

[15] Singh, Karnail B and Tirumkudulu Mahesh S 2007 Cracking in Drying Colloidal Films *Phys. Rev. Lett.* **98**, 218302

[16] Pawar B G, Pinjari P, Divak V K, Sanjay S P, Aniruddha B, and Sung H 2012 *Chemical Enginering* ISRN, 954869, 1-7. DOI: 10.542/2012/954869

[17] Zhao Jun-Hua, Tan Rui-Qin, Yang Ye, Xu Wei, Li Jia, Shen Wen-Feng, Wu Guo-Qiang, Yang Xu-Feng, Song Wei-Jie 2015 Synthesis mechanism of heterovalent Sn_2O_3 nanosheets in oxidation annealing process *Chinese Physics* B Volume **24**, Issue 7, article id. 070505